Desalination 273 (2011) 64–71

Contents lists available at ScienceDirect

Desalination

journal homepage: www.elsevier.com/locate/desal

Mineral scale monitoring for reverse osmosis desalination via real-time membrane surface image analysis

Alex R. Bartman [a], Eric Lyster [a], Robert Rallo [b], Panagiotis D. Christofides [a], Yoram Cohen [a,*]

[a] Department of Chemical and Biomolecular Engineering, University of California, Los Angeles, 420 Westwood Plaza, Chemical Engineering Offices, Boelter Hall 5531, Los Angeles, CA 90095, USA
[b] Department d'Enginyeria Informatica i Matematiques, Universitat Rovira i Virgili, Tarragona, Catalunya, Spain

ARTICLE INFO

Article history:
Received 11 September 2010
Received in revised form 7 October 2010
Accepted 7 October 2010
Available online 30 October 2010

Keywords:
Reverse osmosis
Image analysis
Feed flow reversal
Mineral scaling
Process control

ABSTRACT

An approach to real-time analysis of mineral scale formation on reverse osmosis (RO) membranes was developed using an ex-situ direct observation membrane monitor (MeMo). The purpose of such monitoring is to signal the onset of mineral scaling and provide quantitative information in order to appropriately initiate system cleaning/scale dissolution. The above is enabled by setting the MeMo operating conditions (cross flow velocity and transmembrane pressure) to closely match the conditions in the monitored membrane plant (e.g., in the tail RO element) in order to mimic the surface scaling processes taking place inside the monitored RO plant element. Mineral scale in the MeMo system is monitored by comparison of consecutive images of the membrane surface for the purpose of determining the evolution of the fractional coverage by mineral salt crystals and the corresponding crystal count in the monitored region. Through online image analysis, once crystal growth is determined to be above a prescribed threshold, one can then initiate any number of cleaning protocols. Through early detection of membrane scaling (i.e., before permeate flux decline is observed), enabled by the present monitoring approach, the system operator can prevent irreversible membrane damage and loss of system productivity.

1. Introduction

In recent years, reverse osmosis (RO) desalination has emerged as a leading method for desalting seawater, inland brackish water and water for water reuse applications [1–3]. In inland desalination of brackish water and water reuse, concentrate (brine) management is a major challenge given the limited options for concentrate disposal. With increasing product water recovery, the volume of the residual concentrate stream is reduced, increasing the available options for management of this stream (i.e., treatment and disposal).

Optimal product water recovery levels in brackish water desalting are highly dependent on feed water quality, target production capacity, and locally available options for concentrate disposal. Because the costs associated with managing residual desalination concentrate are typically high (especially at inland locations), high levels of product water recovery (85–95%) are often required for optimal inland desalting operation [4,5]. As the permeate recovery level increases, the level of concentration polarization (i.e., increased solute concentration at the membrane surface relative to the bulk) rises, increasing the propensity for membrane fouling and scaling [6]. Mineral scaling can occur when the concentrations of sparingly soluble dissolved mineral salts (e.g., gypsum ($CaSO_4 \cdot 2H_2O$), $BaSO_4$, $SrSO_4$, $CaCO_3$, SiO_2, etc.) near membrane surfaces rise above their solubility limits. As a consequence, sparingly soluble mineral salts can precipitate in the bulk and subsequently deposit onto the membrane surface as well as crystallize directly on the membrane. Mineral scaling can lead to a significant reduction in membrane performance (e.g., flux reduction and salt rejection impairment) and shortening of membrane life, thereby increasing process cost and imposing operational limits on the achievable product water recoveries [3].

The most common feed water conditioning methods for mitigating mineral scale formation are feed water pH adjustment (primarily for carbonate minerals) and antiscalant treatment [1]. Antiscalant treatment involves dosing of antiscalant chemicals that kinetically delay the onset of mineral salt crystallization and may also retard the growth of mineral salt crystals [7]. The use of antiscalant requires precise knowledge of the optimal antiscalant dose to provide adequate scale protection, decrease process cost associated with antiscalant use, and ensure that excessive antiscalant dosages do not lead to increased scaling or biofouling [8].

If scale formation is detected at an early stage, membrane cleaning can be effectively accomplished via chemical cleaning [9], osmotic backwash [10] or feed flow reversal [11]. Also, conservative operation (i.e., low recovery) can be imposed to ensure that mineral salt concentrations at the membrane surface are below saturation. The

* Corresponding author. UCLA Chemical and Biomolecular Engineering Department, 420 Westwood Plaza, 5531 Boelter Hall, Los Angeles, CA 90095, USA. Tel.: +1 310 825 8766; fax: +1 310 206 4107.
E-mail address: yoram@ucla.edu (Y. Cohen).

0011-9164/$ – see front matter © 2010 Elsevier B.V. All rights reserved.
doi:10.1016/j.desal.2010.10.021

above approaches require knowledge of the scaling propensity for the source water and at the operating conditions (e.g., based on feed water chemistry data or scale monitoring) or real-time membrane monitoring information to detect the onset of mineral scaling. With feed water that may fluctuate in its composition, changes in the level of supersaturation of sparingly soluble mineral salts will also vary with time. Unfortunately, present water quality monitoring capabilities do not provide adequate real-time information on the concentration of mineral salt scale precursors. Therefore, it is imperative to establish when mineral scale may occur and/or directly detect the onset of mineral scaling in order to determine the appropriate frequency of needed membrane cleaning. Early mineral scale detection can also be instrumental in determining required adjustments in operating conditions (e.g., recovery level and antiscalant dose) to ensure process operation below the scaling threshold.

RO systems controller that can respond to changes in feed water salinity and composition have been proposed [12–14; and references therein]. However, even with such systems there is a need for early detection and monitoring of membrane mineral scaling. In-situ monitoring techniques based on indirect ultrasonic crystal detection have been evaluated for the study of mineral scaling and for use in mineral scale and fouling detection in RO systems [6,15–17]. These methods respond to the buildup of a foulant layer but do not differentiate the type of fouling layer (e.g., particulate deposition, bacteria or surface formed crystals) and in general do not detect with sufficient reliability the early onset of membrane surface crystallization (i.e., first formed mineral crystals) [18–20]. In order to accomplish the goal of early mineral scale detection on the membrane surface, a novel ex-situ membrane monitor (MeMo) that enables real-time membrane surface imaging has been recently developed [21,22]. The MeMo detector enables direct observation (i.e., real-time images) of a representative membrane surface where the operating conditions in this ex-situ RO cell are matched to the conditions in the selected spiral-wound element (e.g., tail or lead elements) of the RO plant.

In this work, the application of online imaging of mineral scale formation using the MeMo type system is demonstrated; making use of specialized novel image analysis software for real-time measurement of the fractional area of the membrane surface that is covered by mineral scaling, as well as the number of crystals present on the membrane surface. Using information from real-time mineral scale measurements, it is then possible to automate control actions (e.g., initiation of cleaning strategy, adjustment of antiscalant dose or adjustment of product water recovery) based on a user-defined mineral scaling threshold.

2. Experimental

2.1. Materials

Salt solutions were prepared using calcium chloride ($CaCl_2 \cdot 2H_2O$), barium chloride ($BaCl_2 \cdot 2H_2O$), magnesium sulfate ($MgSO_4 \cdot 7H_2O$), and anhydrous sodium sulfate (Na_2SO_4), all reagent grade obtained from Fisher Scientific (Pittsburgh, PA). The solutions were prepared in de-ionized water obtained by filtering distilled water through a Milli-Q Water System (Millipore Corp., San Jose, CA).

The solution composition for the present study (Table 1) mimicked water composition of primary RO concentrate (salinity of 5219 mg/L total dissolved solids) that would result from desalination of Colorado River water at recovery of 85% [23]. The degree of supersaturation of the various solutions with respect to gypsum ($CaSO_4 \cdot 2H_2O$) and barite ($BaSO_4$) was quantified in terms of the respective saturation indices for these salts (i.e., SI_g and SI_b,):

$$SI_g = \frac{\left(Ca^{2+}\right)\cdot\left(SO_4^{2-}\right)}{K_{sp,g}} \quad , \quad SI_b = \frac{\left(Ba^{2+}\right)\cdot\left(SO_4^{2-}\right)}{K_{sp,b}} \qquad (1)$$

Table 1
Solution composition for membrane scaling experiments.

Ion	Concentration (mg/L)
Na^+	636
Ca^{2+}	681
Mg^{2+}	276
Ba^{2+}	1.2
Cl^-	1206
SO_4^{2-}	2419

where (Ca^{2+}), (Ba^{2+}) and (SO_4^{2-}) are the activities of the calcium, barium and sulfate ions, respectively, and $K_{sp,g}$ and $K_{sp,b}$ are the solubility products for gypsum and barite, respectively. The saturation indices were determined via multi-electrolyte thermodynamic solubility calculations using the OLI Analyzer software [24]. The saturation indices of gypsum and barium sulfate (at 25 °C) for the feed solution (Table 1) were determined to be 0.99 and 156, respectively at the solution pH of ~7. It is noted that, calcium carbonate was not included in the model solution in order to focus on gypsum which is of particular concern in inland water desalination.

The two commercial antiscalants that were used to demonstrate detection capability under the action of scale retardation were PC-504 (Nalco, Naperville, IL) and Flocon 260 (Biolab Water Additives, Tucker, GA), hereinafter referred to as AS1 and AS2, respectively. Ethylenediamine-tetraacetic acid (EDTA, Fisher Scientific, Pittsburgh, PA) was the cleaning agent for the system components. All scaling tests were performed using the TFC-ULP membrane (Koch Membrane Systems, San Diego, CA), reported to have a root mean-square surface roughness of 54.2 nm, $L_p \times 10^7 = 12.3 \pm 0.7$ ($mbar^{-1}\ s^{-1}$) and nominal salt rejection of 97% [23].

2.2. Mineral scale detection system

The membrane monitor (MeMo) used in the present work is similar in construction to the ex-situ scale observation detector (EXSOD) previously developed at UCLA [22,25]. Briefly, the MeMo system consists of a semi-transparent plate-and-frame reverse osmosis cell that allows for real-time imaging of the surface of a membrane coupon placed in the cell. The MeMo cell is comprised of an opaque base with a fritted bottom metal plate to allow the permeate water to channel into the permeate collection tube. The membrane coupon is placed on top of the fritted metal plate; then, several layers of teflon seals are placed around the membrane coupon to allow for high-pressure leak-free operation, as well as to create the feed channel (3.16 cm wide, 8.24 cm long and 2.66 mm in height). A transparent acrylic spacer is placed in between the teflon seals to allow for the entry of the incident light from a direction parallel to the membrane's surface. The acrylic spacer and teflon seals are secured between the base and a thick transparent acrylic block (the top of the cell) which allows for the real-time observation of the membrane surface during system operation. The cell construction allows for operation over a wide pressure range enabling mineral scale monitoring for a wide salinity range (i.e., brackish to seawater). The arrangement of the lighting and feed/retentate streams is shown schematically in Fig. 1. In order to provide proper lighting to enable crystal detection, a line lighting source is fastened to the side of the MeMo cell. Above the cell, a CCD (charge-coupled device) camera attached to a monoscope focuses on a small portion of the membrane coupon surface.

When used as a monitor for a commercial RO plant, feed water to the MeMo cell would be drawn from the high-pressure feed of the tail element of the plant. However, in the present study, a model feed solution (Table 1) was delivered to the MeMo cell from a stirred and temperature controlled (within ±0.5 °C) feed reservoir (18 L), using a high-pressure pump. The feed flow rate is controlled by a pump equipped with a variable frequency drive and also with a bypass valve

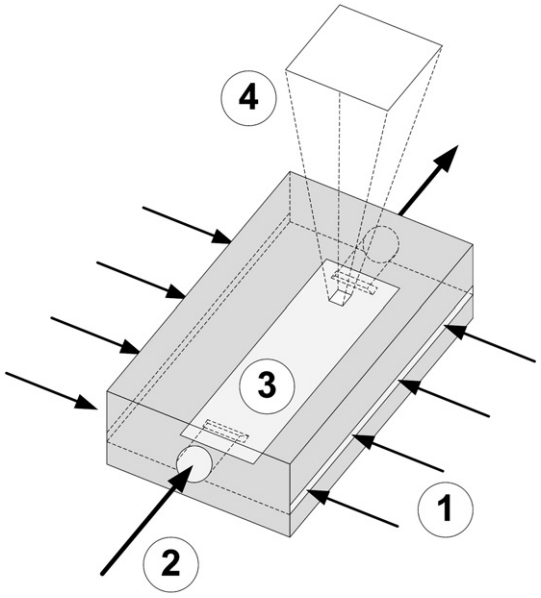

Fig. 1. Membrane monitor (MeMo) cell: 1) Incident light for crystal detection is parallel to the membrane surface, 2) feed water stream entry, 3) membrane coupon underneath transparent top, and 4) example of imaged portion of the membrane surface (size and position can be adjusted).

before the RO cell. Pressure in the cell is adjusted using an actuated valve on the retentate line (located after the MeMo cell). In the present work, the system was operated in a total recycle mode (i.e., permeate and retentate streams continuously recycled to the feed reservoir). As a precautionary measure, a cartridge filter (0.2 μm nominal pore size) was installed on the retentate side of the membrane modules to trap crystals that may have formed in the membrane channel (Fig. 2). Feed flow rate, permeate flux, feed properties (i.e., temperature, pH and salinity) and permeate conductivity were recorded digitally using a computerized data acquisition system as described elsewhere [23].

2.3. Scaling experiments

Prior to each scaling test, a new membrane coupon was conditioned for a period of 4 h by circulating a feed solution composed of all salts except $CaCl_2 \cdot 2H_2O$ and $BaCl_2 \cdot 2H_2O$ through the feed channel with a permeate flux of 36.4 L/m^{2}h (1.2 mL/min permeate flow rate in the present system). Subsequently, predetermined volumes of stock calcium chloride and barium chloride solutions were added to the feed reservoir to obtain the desired feed solution composition (Table 1). All scaling experiments were carried out at 25 °C in a total recycle mode at a cross flow velocity of 4.3 cm/s and an initial permeate flux of 33.4 L/m^{2}h (1.1 mL/min permeate flow rate) ,

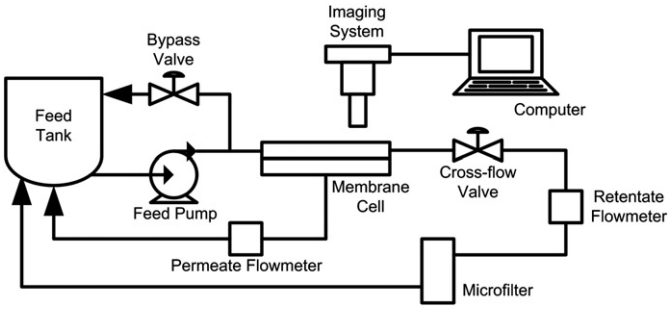

Fig. 2. Schematic of the membrane monitor (MeMo) testing arrangement.

Table 2
List of scaling tests.

Run	Antiscalant	Concentration (ppm)
1	None	0
2	AS1 (PC-504)	1.5
3	AS1 (PC-504)	3
4	AS2 (Flocon 260)	3

with transmembrane pressure typically in the range of 1.03×10^3–1.13×10^3 kPa. At the above conditions, the average initial solution supersaturation indices (SI) at the membrane surface were 2.15 and 403 for gypsum and barite, respectively [23]. It is noted that the SI value for gypsum at the membrane surface was as high as about 2.6 at the channel exit and about 2.2 in the MeMo's imaged region. The above SI values are average values based on the concentration profile determined previously using a 3-dimensional numerical concentration polarization model [26] for the present channel geometry [18] and operating conditions.

Images were collected from four separate experiments with the MeMo system operating at the conditions described above. The feed salt concentrations were identical for all scaling tests which were conducted with and without antiscalant addition to the feed solution (see Table 2).

3. Image analysis

Membrane surface images were captured and stored on the MeMo data acquisition computer at a prescribed interval. During mineral scaling experiments, the MeMo imaging system was set to automatically capture and store an image of the membrane surface at a time interval of 15 min. Upon capture each image was analyzed using imaging processing software developed specifically for the MeMo system. The membrane surface image analysis (MSIA) software consists of the following components; image pre-processing/algorithm initialization, image subtraction and smoothing, edge detection and hysteresis thresholding [27], crystal confirmation and crystal count/area calculation, and data output. A description of the image analysis approach (see Fig. 3) is provided in the following sections.

3.1. Image pre-processing/initialization

The first process in the online image analysis is that of image pre-processing/initialization. In the pre-processing step, the captured color image is converted to an unsigned 8-bit grayscale image. The initialization step involves the creation of a “cumulative scaling image” in order to track the overall growth of the crystals (surface area covered and number of crystals) throughout the course of the experiment. The “cumulative scaling image” is a binary image that is of the same pixel dimensions as the images to be analyzed and is used as a buffer to record confirmed instances of mineral scaling on the membrane surface. Once the presence of a crystal on the membrane surface is confirmed, the corresponding pixels on the cumulative scaling image are changed from 0 to 1. This approach allows for tracking of previously detected crystals and crystals that appear to have stopped growing. Once a new image was analyzed, the updated cumulative image was then used to determine the fractional scale coverage and crystal count during the crystal confirmation, counting, and area calculation step.

3.2. Image subtraction and smoothing

The purpose of the image subtraction step is to determine where crystals have begun to form or have continued growing. This is accomplished by examining a previous image of the membrane and comparing it to a more recent image. Through subtraction of a reference image from the new image, it is possible to determine which

pixels have changed and to what degree; this provides information as to where crystals have formed on the membrane surface. It is noted that subtle changes in lighting or the membrane surface pattern can affect the detection greatly from image to image. The smoothing step is able to decrease the effects of this unwanted "noise" that may lead to false detection of crystals.

In the subtraction step, the new membrane surface image and the reference image (i.e., the membrane surface image preceding the new image) are pre-processed and the absolute difference (necessary to eliminate any bias as to the type of pixel change; darker or lighter) between the images is taken. In this way, the pixels on the images which have changed to the greatest degree become apparent. Image processing filters are then implemented to reduce the impact of possible lighting changes over the course of the experiment.

In the smoothing step, the absolute difference image from the subtraction step is processed using several different methods. First, the analysis applies a Gaussian low-pass filter with properties depending on the crystal type and size in the experiment (determined from preliminary experiments with similar feed water). To smooth the absolute difference image, a convolution of the difference image and of the 2-D Gaussian filter matrix is performed (similar to the procedure of the Canny edge detection method [28]). This Gaussian filter matrix can be represented as:

$$G(x,y) = \frac{1}{2\pi\sigma^2} e^{\frac{-x^2+y^2}{2\sigma^2}} \tag{2}$$

where x and y are the distances from the center of the filter matrix in the horizontal and vertical directions, respectively (the matrix used in this work is a 7×7 matrix, so $x,y|x,y\in\mathbb{Z}$, $|x|,|y|\leq3$), and $\sigma=1$.

3.3. Edge detection and hysteresis thresholding

To determine where crystals have formed on the surface of the membrane, an edge detection algorithm is used to find the outlines of new crystals or to find the areas of growth for existing crystals. After the edge detection algorithm is applied, hysteresis thresholding is carried out to determine which pixels have changed intensity to a sufficient degree to be considered indicative of crystal formation. After converting the original camera image to grayscale, the pixel values are between 0 (black) and 1 (white). During edge detection and hysteresis thresholding, the pixels take on values relative to the largest intensity change that exists in the image (the pixel which has changed the most from the previous image will have a value of 1, and pixels that have not changed have a value of 0). In the next step, the smoothed image is then passed through a function that determines the directional gradients of pixel intensity in the processed image (both in the row and column directions). To find the areas of the image where the directional gradient of the pixel values is greatest, each of the directional gradient matrices are squared (element by element) and added together to form an image highlighting the most prominent edges found on the original image. From the resulting image, the pixels where the greatest change in intensity has occurred and the crystal edges can be observed.

Subsequently, hysteresis thresholding is conducted, making use of preset upper and lower thresholds. The upper threshold, denoted as "UT", is used to locate the most prominent changes in pixel value in the processed image; any pixels which have a value larger than the upper threshold are flagged as possible scale pixels. The algorithm then scans any pixels directly connected to the flagged pixels and also flags any of these pixels that have values above the lower threshold (denoted as "LT"). After the corresponding pixels on the binary matrix are marked, the image undergoes several morphological cleaning and filling operations in order to remove isolated pixels (e.g., single flagged pixels surrounded by eight un-flagged pixels, tending to be a false positive) and also to fill in "holes" (e.g., un-flagged pixels surrounded by eight flagged pixels).

3.4. Crystal confirmation, counting and area determination

Prior to calculating the surface coverage and number of crystals are the flagged pixels are checked against previously flagged pixels on the cumulative scaling image in order to determine whether or not the newly detected pixels are actually an instance of scaling, or a false positive detection. If a flagged pixel is located in the same spot as in the previous image comparison, then this pixel can be considered to be confirmed scaling. It is also noted that a "confirmation threshold" can be set to allow the user to control how stringent the software will be in confirming the location and amount of scale formed. If the confirmation threshold is preset to a value of 1, this means that a flagged pixel must persist in two consecutive image analyses in order to be considered as scale formation and added to the cumulative scaling image. In systems where the lighting is stable and provides excellent contrast between the membrane and the crystal, this confirmation threshold can be set to zero. For the results presented in this work, the confirmation threshold was set to a value of 2.

Since the cumulative scaling image contains only ones and zeros, the flagged pixels are summed and divided by the total number of pixels in the image, resulting in the fraction of the image covered by flagged scaling pixels. This value is then passed to the graphical user interface (GUI) and plotted so that the user can see the real-time update of the surface coverage vs. time (or image number). The cumulative scaling image is also used in the algorithm to determine the number of crystals present on the membrane surface (this metric can also be used to trigger membrane cleaning). In the crystal count algorithm, the flagged pixel groups are screened using several methods; the first one being an area thresholding process. In this process, crystals with an area smaller than a threshold value are not counted as crystals. Moreover, initially identified potential crystals that did not grow to sizes above the minimum threshold over the course of the experiment were removed from the crystal count and scaled area calculation. For experiments resulting in a smaller number of large crystals (runs 1 and 2), a typical threshold of 350 pixels was set (each pixel representing an area of 3×10^{-5} cm^2), corresponding to a surface coverage value of about 0.02%. For scaling experiments resulting in a larger number of small crystals, the threshold value was set lower (i.e., 175 pixels for run 3, and 150 pixels for run 4). Subsequent to the area thresholding, a grouping algorithm is applied to the cumulative scaling image. In this procedure, pixels marked as crystals within a predetermined proximity of other marked pixels are grouped together and considered as part of the same crystal. This pixel proximity distance is based on the average radius of crystals when they are first observed. In this work, the proximity distance of 4 pixels was found to be adequate.

3.5. Manual image analysis

After the completion of a given scaling experiment, manual image analysis was conducted for selected captured images using the MSIA software for comparison with the automated real-time image analysis software developed for the MeMo system. From the experimental data, the surface coverage was determined "manually" using digital image analysis software (Fovea plug-in for Adobe Photoshop) as discussed in [8]; each individual crystal in the images was outlined by hand and colored (e.g., red), then, built in functions were used to determine the surface area covered by these crystals, as well as the total number of crystals present in each image. Clearly, the above "manual" image analysis method would be intractable for large sets of images and thus demonstrates the need for the automated image analysis employed in the present work.

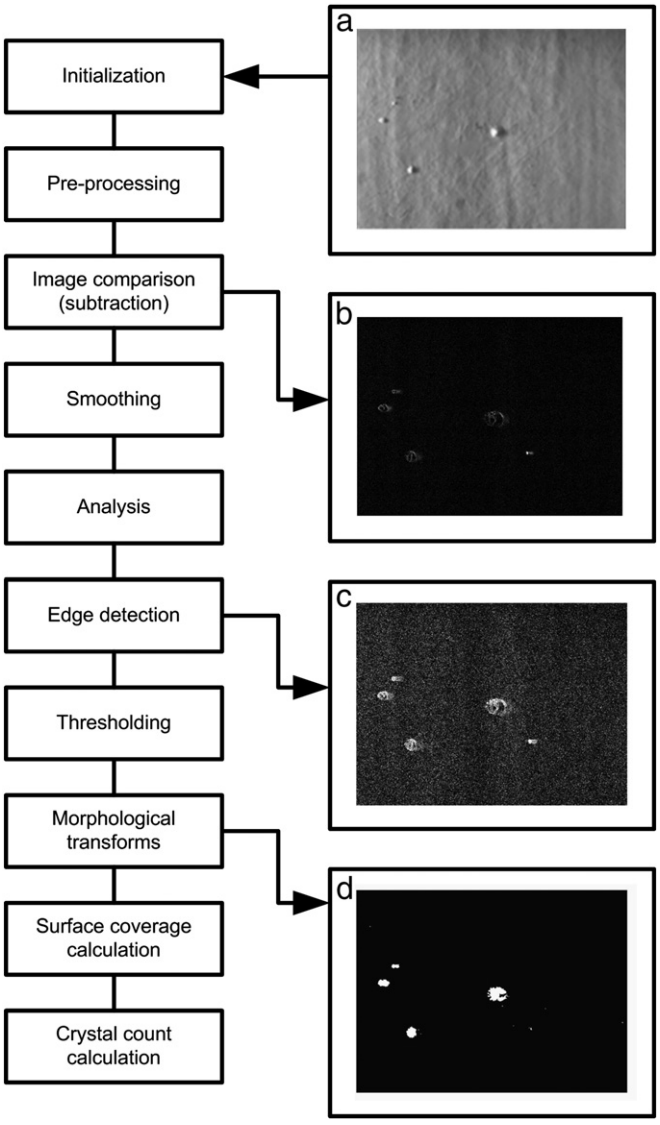

Fig. 3. Flowchart of image analysis algorithm with representative example image outputs for selected algorithm steps: a) original camera image saved to MeMo computer disk, b) image resulting from subtraction of two most recently captured images (black pixels represent little to no change in pixel value and white denotes large changes when compared to the previous image), c) subtracted image after image filtering and edge detection, and d) final cumulative scaling image after morphological transforms.

4. Results and discussion

4.1. Mineral scale surface coverage

The performance of the online surface scale image analysis is illustrated in Figs. 4–7 for the scaling runs without and with antiscalant addition, respectively. The percent of surface coverage by mineral scale as determined by online automated image analysis follows the manual image analysis reasonably well, with a maximum deviation of about 3%. Agreement between the manual and automated image analysis was excellent at the early stages of scale development (when less than about 10% of the surface in the monitored area was covered by scale). These early stages of detection are most critical since scale mitigation actions (e.g., increasing antiscalant dose, initiation of membrane cleaning or adjustment of operating conditions) would most likely be desired early in the membrane scaling process [18]. Although membrane images were analyzed until membrane surface coverage reached approximately 15–25%, at this

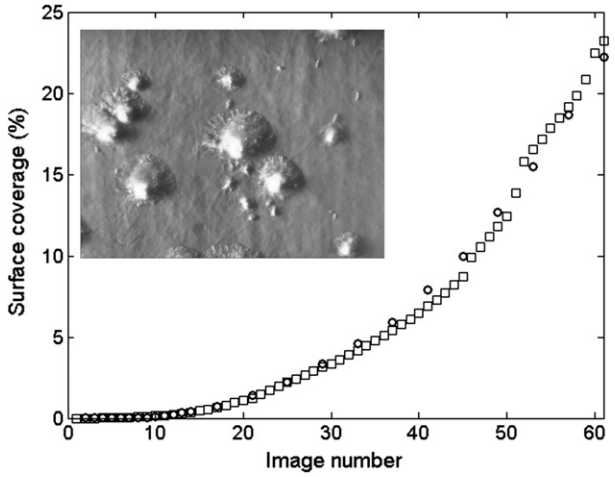

Fig. 4. Percentage of mineral scaled membrane area (in the MeMo monitored) obtained via "manual" image analysis (circles) and MeMo automated scale detection software (squares) for Run 1 (without antiscalant addition; Table 2) with threshold tolerances UT = 0.54, LT = 0.59, and minimum crystal size of 350 pixels. Inset shows membrane surface image 61. (Images captured and analyzed every 15 min).

high level of surface scale buildup significant flux decline would be expected when monitoring the tail membrane element of RO plants [23] which could possibly lead to membrane damage. The rate of surface mineral scaling decreased with the application of 3 ppm of antiscalant AS2 (run 4, Fig. 7) with scale coverage of 15% reached in 260 h (image 29). In contrast, doses of 1.5 ppm AS1 (run 2) and 3 ppm AS1 (run 3) were insufficient to retard gypsum scaling with 15% surface coverage reached within 7.25 h and 5.25 h, respectively, similar to the run without antiscalant dosing. The above results demonstrate that, in addition to monitoring mineral scaling, the MeMo system can also be used to assess antiscalant effectiveness in suppressing mineral scaling.

The crystal size and shapes can vary depending on the antiscalant type and dose (Table 2) as illustrated by the image insets in Figs. 4–7. Also, given the three-dimensional nature of surface crystals, the ability to detect crystal edges may be influenced by shadows and effect of neighboring crystals. Notwithstanding, in the present work a single set of UT and LT settings for a given scaling experiment were found sufficient to provide a reasonable level of mineral scale detection accuracy. It is acknowledged, however, that for a broader

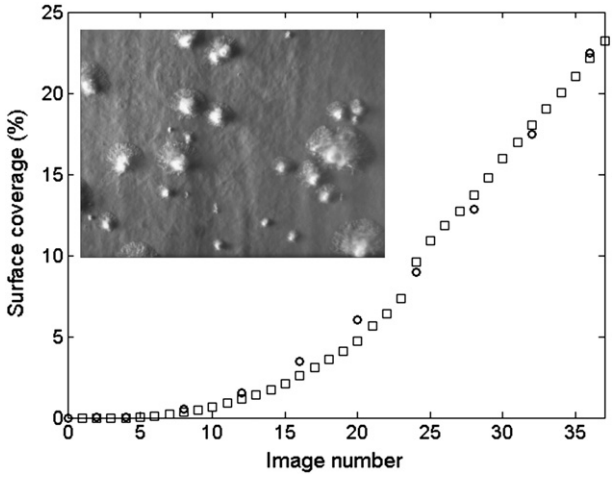

Fig. 5. Percentage of mineral scaled membrane area (in the MeMo monitored) obtained via "manual" image analysis (circles) and MeMo automated scale detection software (squares) for Run 2 (1.5 ppm of AS1; Table 2) with threshold tolerances UT = 0.42, LT = 0.43, and minimum crystal size of 350 pixels. Inset shows membrane surface image 37. (Images captured and analyzed every 15 min).

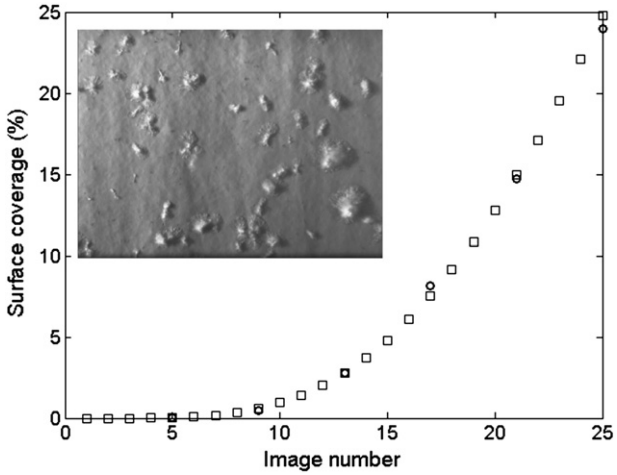

Fig. 6. Percentage of mineral scaled membrane area (in the MeMo monitored) obtained via "manual" image analysis (circles) and MeMo automated scale detection software (squares) for Run 3 (3 ppm of AS1; Table 2) with threshold tolerances UT = 0.36, LT = 0.49, and minimum crystal size of 175 pixels. Inset shows membrane surface image 25. (Images captured and analyzed every 15 min).

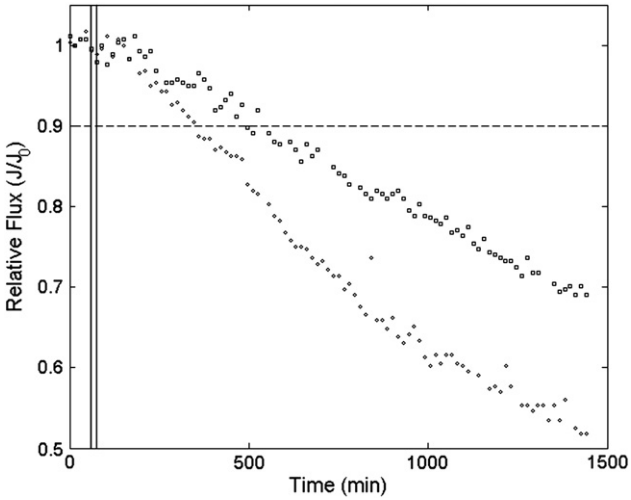

Fig. 8. Relative permeate flux vs. time for run 1 (squares; without antiscalant) and run 3 (diamonds; 3 ppm AS1). The dashed horizontal line represents a 10% decline in permeate flux from the original flux at the start of the scaling experiments. The vertical lines represent the first detection of mineral salt scaling by the MSIA for runs 1 and 3 (at 60 and 75 min, respectively).

range of application of the MeMo system the hysteresis threshold tolerances (UT and LT, Section 3.3) may have to be adjusted over the course of monitoring via automated image calibration, for the specific lighting conditions and type of surface crystal topography.

Early scale detection, while avoiding false positive crystal detection, prior to the observation of measurable permeate flux decline was demonstrated for two scaling experiments with (run 3, 3 ppm AS1) and without (run 1) antiscalant addition. Membrane surface monitoring in the MeMo cell (in the region near the channel exit) revealed significant scale (Figs. 4, 6), before any measurable flux decline (Fig. 8). It is apparent that the surface coverage and crystal counts for runs 1 and 3 (Figs. 4, 6, 9, and 11) track very closely with the manual analysis, demonstrating the avoidance of false positive detection. Even though the surface coverage analysis is of sufficient accuracy depending on the feed solution characteristics and the type of additives present, it may be desirable to monitor the number of crystals present on the membrane surface since early detection of mineral crystals is even more pronounced via the monitored crystal count as discussed in Section 4.2.

4.2. Crystal identification and crystal count

Crystal count was performed once crystals were identified as described in Section 3 (results shown in Figs. 9–12). It is important to recognize that identification of the first crystal was achieved (Figs. 9, 11) before the detection of any measurable flux decline (Fig. 8). The first crystals were detected (in runs 1 and 3) between 60 and 75 min after the start of the experiment, while the permeate flux was still between 96 and 100% of the original flux. By the time the permeate flux has decreased to measurable levels (~10% flux decline), multiple crystals were already visible on the membrane surface. The crystal count also shows good agreement with the "manually" determined crystal count, with a maximum deviation of about 6 crystals between the MSIA result and the "manual" count. It is also noted that this

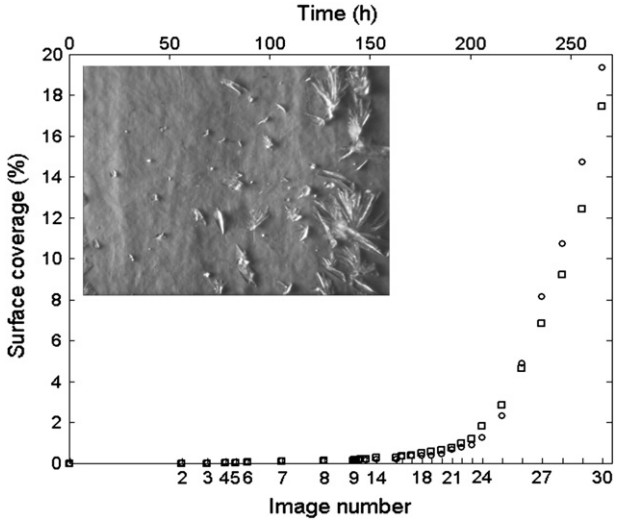

Fig. 7. Percentage of mineral scaled membrane area (in the MeMo monitored) obtained via "manual" image analysis (circles) and MeMo automated scale detection software (squares) for Run 4 (3 ppm of AS2; Table 2) with threshold tolerances UT = 0.68, LT = 0.71, and minimum crystal size of 150 pixels. Inset shows membrane surface image 30. (Note: The capture time for the analyzed images is indicated in the top horizontal axis.)

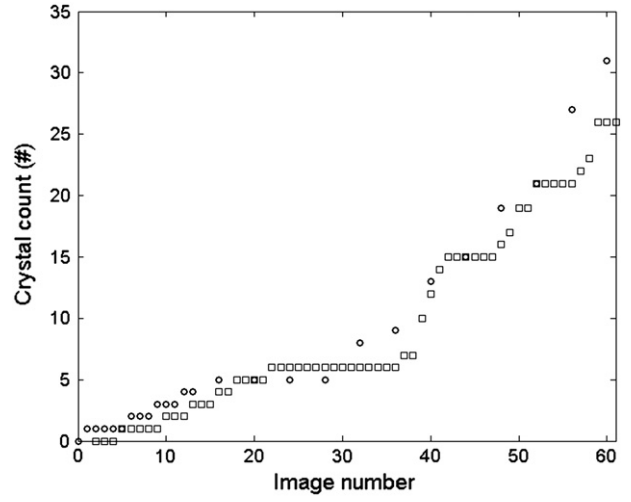

Fig. 9. Crystal count in the MeMo monitored membrane area obtained from both manual (circles) and automated scale detection (squares) for Run 1 (without antiscalant addition; Table 2) where UT = 0.54, LT = 0.59, and minimum crystal size of 350 pixels. (Images captured and analyzed every 15 min).

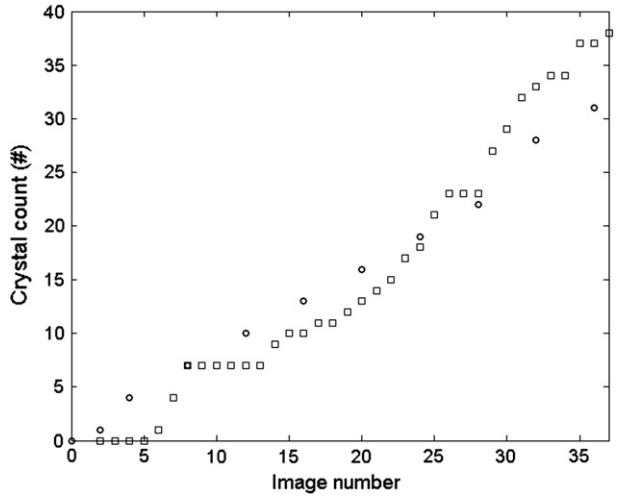

Fig. 10. Crystal count in the MeMo monitored membrane area obtained from both manual (circles) and automated scale detection (squares) for Run 2 (1.5 ppm antiscalant AS1; Table 2) where UT = 0.42, LT = 0.43, and minimum crystal size of 350 pixels. (Images captured and analyzed every 15 min).

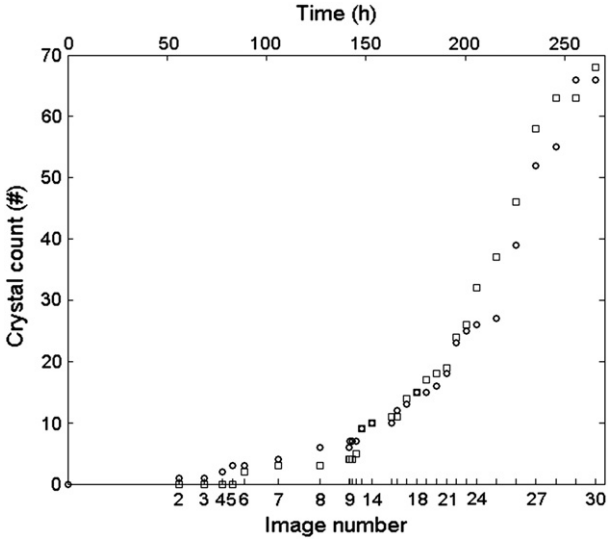

Fig. 12. Crystal count in the MeMo monitored membrane area obtained from both manual (circles) and automated scale detection (squares) for Run 4 (3 ppm antiscalant AS2; Table 2) where UT = 0.68, LT = 0.71, and minimum crystal size of 150 pixels. (Note: The capture time for the analyzed images is indicated in the top horizontal axis).

maximum deviation occurs when many crystals are present on the membrane surface; the MSIA crystal count is much more accurate at the beginning of the scaling process when critical control decisions must be made (e.g., to activate a cleaning process or change operating conditions to avert flux decline).

Scale monitoring using the MeMo device can be particularly useful for evaluating antiscalant effectiveness [29] and for triggering RO scale mitigation actions as recently demonstrated for the present system for RO plant operation in feed flow reversal mode [18]. In such applications, appropriate automation is required to enable adjustment of the pressure and flow rate in the MeMo RO cell so as to match the condition of solution supersaturation at the membrane surface to that in the RO plant element being monitored [18]. The MeMo device can also be used in a stand-alone mode (i.e., prior to its connection as an online detector) to determine the operational parameters that lead to scaling [18,19,30]. Such information can provide knowledge of the operational region(s) that would result in mineral scaling and also allow one to arrive at optimal image analysis settings to enhance scale detection.

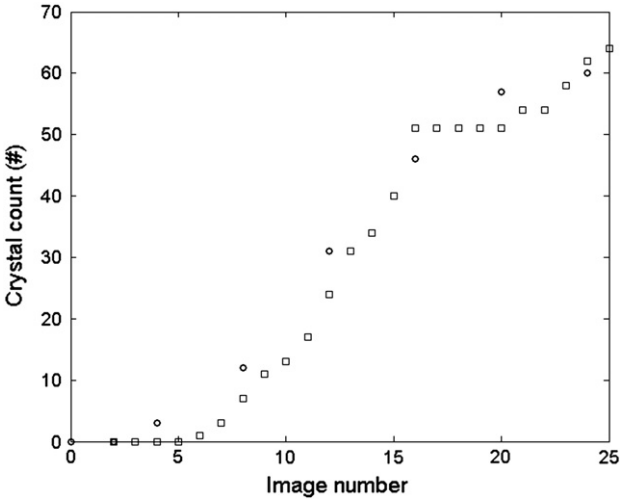

Fig. 11. Crystal count in the MeMo monitored membrane area obtained from both manual (circles) and automated scale detection (squares) for Run 3 (3 ppm antiscalant AS1; Table 2) where UT = 0.36, LT = 0.49, and minimum crystal size of 175 pixels. (Images captured and analyzed every 15 min).

5. Conclusions

An approach to real-time analysis of the formation of mineral scale on reverse osmosis (RO) membranes was developed using an ex-situ direct observation membrane monitor (MeMo). Real-time images of the membrane surface in the MeMo membrane channel were analyzed online to detect the onset of mineral crystals and to monitor the evolution of the fractional coverage by mineral salt crystals and crystal count. Image analysis software, which was developed specifically for the MeMo system, was capable of real-time detection of the formation and growth of mineral crystals on the membrane surface. The automated image analysis program (operating either online, or in a post-processing mode) was shown to accurately determine the membrane surface coverage by mineral salt scaling and the number of crystals present in the observation area of the detector. With the present scale monitoring approach, when mineral scale coverage reaches a prescribed threshold, a control signal can be sent to the plant control system in order to initiate any number of cleaning protocols. In addition to potential applications for RO plant monitoring, the present monitoring system with its automated surface analysis software can serve to acquire information regarding mineral scale kinetics (e.g., rate of nucleation and rate of growth of individual crystals) and to evaluate the suitability of other scale measures (e.g., geometrical measures of crystal shape and crystal number density) for optimal control strategies.

Acknowledgements

This work was supported, in part, by the California Department of Water Resources, the Office of Naval Research, the United States Environmental Protection Agency and a fellowship to Mr. Eric Lyster from the National Water Research Institute. Also acknowledged is support received by Robert Rallo from the CICYT (CTQ2009-15627).

References

[1] A. Rahardianto, J. Gao, C.J. Gabelich, M.D. Williams, Y. Cohen, High recovery membrane desalting of low-salinity brackish water: integration of accelerated precipitation softening with membrane RO, J. Membr. Sci. 289 (2007) 123–137.
[2] I.C. Karagiannis, P.G. Soldatos, Water desalination cost literature: review and assessment, Desalination 223 (2008) 448–456.

[3] M. Gloede, T. Melin, Physical aspects of membrane scaling, Desalination 224 (2008) 71–75.
[4] C.J. Gabelich, T.I. Yun, B.M. Coffey, I.H. Suffet, Pilot-scale testing of reverse osmosis using conventional treatment and microfiltration, Desalination 154 (2003) 207–223.
[5] A. Zhu, P.D. Christofides, Y. Cohen, Effect of thermodynamic restriction on energy cost optimization of RO membrane water desalination, Ind. Eng. Chem. Res. 48 (2009) 6010–6021.
[6] Z. Zhang, V.M. Bright, A.R. Greenberg, Use of capacitive microsensors and ultrasonic time-domain reflectometry for in-situ quantification of concentration polarization and membrane fouling in pressure-driven membrane filtration, Sens. Actuator B 117 (2006) 323–331.
[7] R.Y. Ning, T.L. Troyer, R.S. Tominello, Chemical control of colloidal fouling of reverse osmosis systems, Desalination 172 (2005) 1–6.
[8] A. Rahardianto, W. Shih, R. Lee, Y. Cohen, Diagnostic characterization of gypsum scale formation and control in RO membrane desalination of brackish water, J. Membr. Sci. 279 (2006) 655–668.
[9] W.S. Ang, S. Lee, M. Elimelech, Chemical and physical aspects of cleaning organic-fouled reverse osmosis membranes, J. Membr. Sci. 272 (2006) 198–210.
[10] N. Avraham, C. Dosoretz, R. Semiat, Osmotic backwash process in RO membranes, Desalination 199 (2006) 387–389.
[11] A.R. Bartman, C.W. McFall, P.D. Christofides, Y. Cohen, Model predictive control of feed flow reversal in a reverse osmosis desalination process, J. Proc. Cont. 19 (2008) 433–442.
[12] A.R. Bartman, P.D. Christofides, Y. Cohen, Non-linear model-based control of an experimental reverse-osmosis water desalination system, Ind. Eng. Chem. Res. 48 (2009) 6126–6136.
[13] J.Z. Assef, J.C. Watters, P.B. Deshpande, I.M. Alatiqi, Advanced control of a reverse osmosis desalination unit, J. Proc. Cont. 7 (1997) 283–289.
[14] A. Abbas, Model predictive control of a reverse osmosis desalination unit, Desalination 194 (2006) 268–280.
[15] J.C. Chen, Q. Li, M. Elimelech, In situ monitoring techniques for concentration polarization and fouling phenomena in membrane filtration, Adv. Colloid Interface Sci. 107 (2004) 83–108.
[16] C.A.C. van de Lisdonk, J.A.M. van Paassen, J.C. Schippers, Monitoring scaling in nanofiltration and reverse osmosis membrane systems, Desalination 132 (2000) 101–108.
[17] E. Kujundzic, K. Cobry, A.R. Greenberg, M. Hernandez, Use of ultrasonic sensors for characterization of membrane fouling and cleaning, J. Eng. Fibers Fabr. 3 (2008) 35–44.
[18] M. Uchymiak, A. Rahardianto, E. Lyster, J. Glater, Y. Cohen, A novel RO ex situ scale observation detector (EXSOD) for mineral scale characterization and early detection, J. Membr. Sci. 291 (2007) 86–95.
[19] M. Uchymiak, E. Lyster, J. Glater, Y. Cohen, Kinetics of gypsum crystal growth on a reverse osmosis membrane, J. Membr. Sci. 314 (2008) 163–172.
[20] A.P. Mairal, A.R. Greenberg, W.B. Krantz, L.J. Bond, Real-time measurement of inorganic fouling of RO desalination membranes using ultrasonic time-domain reflectometry, J. Membr. Sci. 159 (1999) 185–196.
[21] E. Lyster, Y. Cohen, Numerical study of concentration polarization in a rectangular reverse osmosis membrane channel: permeate flux variation and hydrodynamic end effects, J. Membr. Sci. 303 (2007) 140–153.
[22] M. Uchymiak, A.R. Bartman, N. Daltrophe, M. Weissman, J. Gilron, P.D. Christofides, W.J. Kaiser, Y. Cohen, Brackish water reverse osmosis (BWRO) operation in feed flow reversal mode using an ex situ scale observation detector (EXSOD), J. Membr. Sci. 341 (2009) 60–66.
[23] M. Kim, J. Au, A. Rahardianto, J. Glater, Y. Cohen, F.W. Gerringer, C.J. Gabelich, Impact of conventional water treatment coagulants on mineral scaling in RO desalting of brackish water, Ind. Eng. Chem. Res. 48 (2009) 3126–3135.
[24] OLI Systems, 2.0, OLI Analyzer, Morris Plains, NJ, 2005.
[25] Y. Cohen, M. Uchymiak, Method and system for monitoring reverse osmosis membranes, Patent Pending, WO 2007/087578.
[26] E. Lyster, J. Au, R. Rallo, F. Giralt, Y. Cohen, Coupled 3-D hydrodynamics and mass transfer analysis of mineral scaling-induced flux decline in a laboratory plate-and-frame reverse osmosis membrane module, J. Membr. Sci. 339 (2009) 39–48.
[27] P. Kovesi, hystresh.m, School of Computer Science & Software Engineering, University of Western Australia, Copyright © 1996–2005.
[28] J. Canny, A computational approach to edge detection, IEEE Trans. Pattern Anal. Mach. Intell. 8 (1986) 679–698.
[29] E. Lyster, M. Kim, J. Au, Y. Cohen, A method for evaluating antiscalant retardation of crystal nucleation and growth on RO membranes, J. Membr. Sci. 364 (2010) 122–131.
[30] A. Rahardianto, B.C. McCool, Y. Cohen, Reverse osmosis desalting of inland brackish water of high gypsum scaling propensity: kinetics and mitigation of membrane mineral scaling, Environ. Sci. Technol. 42 (2008) 4292–4297.